COVID-19 Associated Rhino-Orbito-Cerebral Mucormycosis : A Single Tertiary Care Center Experience of Imaging Findings in COVID-19 Associated Mucormycosis with A Special Focus on the Intracranial Manifestations of Mucormycosis.

Megha Gireesan Nair (meghagiresan5@gmail.com)
Seth Gordhandas Sunderdas Medical College: King Edward Memorial Hospital and Seth Gordhandas Sunderdas Medical College https://orcid.org/0000-0002-4311-429X

Shilpa Sankhe Susheelkumar
Seth Gordhandas Sunderdas Medical College: King Edward Memorial Hospital and Seth Gordhandas Sunderdas Medical College

Gayatri Autkar M
Seth Gordhandas Sunderdas Medical College: King Edward Memorial Hospital and Seth Gordhandas Sunderdas Medical College

Research Article

Keywords: Mucormycosis, COVID-19, Imaging findings, Rhinocerebralmucormycosis, Black Fungus, rhino-orbito-cerebral.

Posted Date: February 25th, 2022

DOI: https://doi.org/10.21203/rs.3.rs-1343008/v1

Abstract

Context: The current COVID-19 pandemic and mucormycosis epidemic in India has made research on radiological findings of COVID-19 associated mucormycosis imperative.

Aim: To describe the imaging findings in COVID-19 associated mucormycosis with a special focus on the intracranial manifestations.

Materials and methods: MRI scans of all patients with laboratory proven mucormycosis and post COVID-19 status, over a period of two months, at an Indian Tertiary Care Referral Centre, were retrospectively reviewed and descriptive statistical analysis was carried out.

Results: 58 patients (47 men and 11 women) were evaluated. Deranged blood glucose levels were observed in 81% of cases. Intracranial invasion was detected in 31 patients (53.4%). The most common finding in cases with intracranial invasion was pachymeningeal enhancement (90.3% i.e., 28/31). This was followed by infarcts (17/31 i.e., 55%), cavernous sinus thrombosis (11/58 i.e., 18.9%), fungal abscesses (11/31 i.e., 35.4%), and intracranial hemorrhage (5/31 i.e., 16.1% cases). Perineural spread was observed in 21.6% (11/51) cases.

Orbital findings included extraconal fat and muscle involvement, intraconal involvement, orbital apicitis, optic neuritis, panophthalmitis, and orbital abscess formation in decreasing order of frequency. Cohen's kappa coefficient of inter-rater reliability for optic nerve involvement and cavernous sinus thrombosis was 0.7. Cohen's coefficient value for all other findings was 0.8-0.9.

Conclusions: COVID-19 associated Rhinocerebral mucormycosis has a plethora of orbital and intracranial manifestations. MRI, with its superior soft-tissue resolution, is the imaging modality of choice to expedite the initial diagnosis, accurately map out disease extent, and for prompt identification and scrupulous management of its complications.

Introduction

COVID-19 pandemic has ravaged most nations across the world. [1] Following the second wave [2] however, there has been a cascade of Mucormycosis cases in India. This previously uncommon fungal infection explosively increased in numbers. Filamentous fungi that belong to the subphylum Mucoromycotina [3] and order Mucorales [4] cause an invasive disease, which may involve multiple systems; namely, the paranasal sinuses, the orbits, the central nervous system, musculoskeletal system, [5] lungs, gastrointestinal tract, and even the liver. [4] This is denoted by the term "mucormycosis". It is often called Rhino-orbito-cerebral mucormycosis based on the most frequently invaded organs. [3] Mucormycosis is already the most rapidly fatal fungal infection in human beings. [6] This study is an attempt to explore and objectively characterize the imaging manifestations in laboratory-confirmed cases of COVID-19 associated rhino-cerebral mucormycosis. [7]

Methods

This study included 58 laboratory-confirmed cases of COVID-19 associated Rhinocerebral mucormycosis, fulfilling the inclusion criteria, who underwent contrast-enhanced MRI at our institute between 15 March 2021 and 15 November 2021.

Institutional review board and Institutional ethics committee approval were obtained for this retrospective study. We reviewed patients' imaging studies and departmental records. Consent waiver was granted by the institutional ethics committee in view of its retrospective nature.

Imaging Technique:

The standard protocol followed at our institute for suspected or diagnosed cases of mucormycosis was adhered to. MRI was performed on a Siemens Magnetom Aera 1.5-T magnet with a 48-channel head coil equipped with array spatial sensitivity encoding and parallel acquisition. Our standard orbit with paranasal sinus and brain MRI protocol includes whole-brain axial turbo spin-echo T2 weighted sequence, FLAIR (Fluid attenuated inversion recovery) coronal, axial Susceptibility-weighted (SWI), T1 weighted non-fat saturated sagittal, Diffusion-Weighted Imaging (DWI) B1000, and generating trace and ADC (apparent diffusion coefficient maps). Axial and coronal brain T1 fat-saturated contrast-enhanced sequences were also acquired. High-resolution orbit sequences include fast spin-echo axial T2, unenhanced T1 axial, contrast-enhanced T1 axial, and coronal images also covering the paranasal sinuses. Post-contrast MPRAGE sequence was also acquired. Time of flight (TOF) brain and neck angiography was performed in patients showing infarcts or abnormal ICA (internal carotid artery) flow voids. We used a standard dose of 0.1 mmol/kg of gadoterate meglumine, intravenous contrast material (Dotarem, Guerbet). In patients with intracranial hemorrhage, the protocol was extended to include MRI venography.

Inclusion criteria:

1. Patients with documented RT-PCR (Reverse transcriptase-polymerase chain reaction) positive status within the past two months.

2. Patients with laboratory-proven mucormycosis either on KOH (Potassium hydroxide) mount or fungal culture or histopathology.

Exclusion criteria:

1. Patients who had undergone treatment including debridement or medical management before imaging.

2. Scans of suboptimal quality due to artifacts.

Aims and objectives:

- To describe the imaging findings in COVID-19 associated rhinocerebral mucormycosis with a special focus on the intracranial manifestations.
- To determine the interrater reliability of the various parameters used in the evaluation of rhinocerebral mucormycosis.

Image analysis:

The studies were reviewed independently on a Siemens Syngo standalone viewer, version: VD11 (Erlangen, Germany) by 2 qualified radiologists with three years and five years of experience respectively, and disagreements were resolved independently by a third senior radiologist with 15 years of experience. CT data of these patients was retrospectively analyzed only to evaluate bone involvement or to look for the presence of hemorrhage.

We followed a structured reporting format [Table 1] in all cases of COVID-19 associated mucormycosis.

The maxillary, ethmoid, sphenoid, and frontal sinuses were evaluated for mucosal thickening, altered signal intensity, and post-contrast enhancement. The turbinates were also evaluated for altered signal intensity on non-contrast MRI images and then for presence or absence of post-contrast enhancement. Lamina papyracea, cribriform plate, sphenoid bone, and pterygoid plates were also similarly evaluated. CT images were retrospectively evaluated for all cases to assess the presence of bone erosions or rarefaction, indicating the involvement of the bony structures mentioned above.

Pterygomaxillary fissure, pterygopalatine fossa, retro-antral fat, masticator space muscles, and subcutaneous tissues were evaluated for altered signal intensity and for post-contrast enhancement.

The extra-ocular muscles were evaluated for T2/FLAIR hyperintensity and increase in muscle bulk as well as with post-contrast enhancement. The extra-conal fat was also evaluated for T2/FLAIR hyperintensity and post-contrast enhancement. Intraconal fat, orbital apex were also evaluated for the presence or absence of enhancing soft tissue.

Non-contrast and contrast-enhanced sequences of brain MRI were evaluated in detail, for all suspected complications. Both source images, as well as MIP images of TOF angiography, were evaluated.

Criteria used to evaluate various complications of Rhino-orbito-cerebral mucormycosis are elaborated in Table 2.

Table 1

Sr no.		Structured reporting format:	RIGHT	LEFT
1.	Paranasal Sinuses: Mucosa and contents	a) Maxillary sinus		
		b) Ethmoid sinus		
		c) Sphenoid sinus		
		d) Frontal sinus		
2.	Nasal Turbinates:	Post contrast enhancement pattern		
3.	Orbit:	a) Extraconal fat involvement		
		b) Extraocular muscle involvement		
		c) Intraconal fat involvement		
		d) Optic nerve involvement		
		e) Orbital apex involvement		
		f) Superior orbital fissure & Inferior orbital fissure		
4.	Masticator space involvement:	a)Retroantral fat pad involvement		
		b)Pterygopalatine fossa involvement/ Pterygomaxillary fissure		
		c)Subcutaneous tissues: Premaxillary region / preseptal space orbit		
		d) Muscles of masticator space		
5.	Perineural spread assessment:	Foramen ovale / Foramen rotundum/ Vidian canal		
6.	Bone involvement:			
7.	Intracranial involvement:	Cavernous sinus thrombosis		
		Internal carotid artery: Patent/ Narrowed/ Thrombosed		
		Meningeal inflammation		
		Extra-axial space: Abscess/ hematoma.		
		Brain parenchyma: Cerebritis/ Abscess/ Infarcts/ Hematoma		
8.	Brain angiography:	Vessel narrowing/ thrombosis/ mycotic aneurysm		

Table 2: Imaging appearance of various complications of Rhino-orbito-cerebral mucormycosis

Complication:	Imaging appearance:
Cavernous sinus thrombosis	Presence of convex outer walls. Abnormal signal intensity on plain MRI. Post contrast images were assessed for any filling defect within the sinus and presence of abnormal dural enhancement along its lateral wall.
Angioinvasive disease involving Internal carotid artery	T2 hyperintensity of wall with wall thickening, enhancement, narrowing and luminal irregularity involving the internal carotid artery
Mycotic aneurysm	Eccentric saccular or fusiform aneurysm with changes of vasculitis or enhancing soft tissue surrounding it.
Panophthalmitis	Abnormal shape of eyeball with diffusion restriction within the posterior coats as well as heterogenous contents in eyeball.
Optic nerve Involvement	Swelling of the optic nerve with obliteration of the CSF sleeve and T2/FLAIR hyperintense signal with post contrast enhancement.
Perineural spread	Thickening of the nerve, widening of the adjacent neural foramen and enhancement along the nerve.

< Table 3: Intracranial invasion >

Criteria:	Number of patients:	Percentage:
Total number of patients	58	Percentage of total
Number of patients with intracranial invasion	31	53%
Pachymeningeal enhancement	28	48%
Cavernous sinus thrombosis	11	18.90%
Internal Carotid artery involvement	11	19%
Internal carotid artery thrombosis	8	13.70%
Internal carotid artery wall thickening, enhancement and narrowing	3	5.10%
Infarcts	17	29%
Watershed territory infarcts	4	6.90%
Vasculitic/embolic infarcts	12	20.6
Extra-axial Hemorrhage	2	3.40%
Intraparenchymal Hemorrhage	4	6.90%
Fungal intraparenchymal abscess	7	12.00%
Fungal extra-axial abscess	5	8.60%
Mycotic aneurysm	2	3.40%
Intraventricular Exudate	2	3.40%

Statistical analysis:

Statistical analysis was performed using the IBM SPSS Statistics software version: 27.0/ June 19, 2020 (IBM, New York USA).

The numerical data has been analyzed and expressed as mean and standard deviation and range. Ratios, proportions, and percentages were derived for categorical and nominal data. Interrater agreement was also assessed for the two primary reviewers. Cohen's kappa coefficient was assessed. The interpretation of Cohen's kappa coefficient was as follows: values ≤ 0 as indicating no agreement and 0.01–0.20 indicates no to slight agreement, 0.21–0.40 indicates fair agreement, 0.41– 0.60 as moderate agreement, 0.61–0.80 as substantial agreement, and 0.81–1.00 as near-perfect agreement. [8]

Results

Demographic and clinical characteristics:

A total of 58 cases fulfilling the inclusion criteria were selected for the study. The mean age of the study population was 49.2 Years (Range: 18-77 Years). Standard Deviation was 12.7 years. The ratio of Male: Female patients was 47:11 that is 81% of patients were men and 19% were women.

Age-wise distribution of patients is described in Supplementary Figure 1.

Clinical history and laboratory findings:

All of the patients included in the study had documented evidence of previous COVID-19 positive status on RT-PCR. All patients included in the study also had laboratory documented evidence of mucormycosis on either KOH mount or culture or histopathological analysis.

Amongst the patients included in the study, 37 patients (64%) were known diabetics and the rest had no documented evidence of deranged blood sugars or diabetes before the COVID-19 episode. One patient was a case of renal transplantation on immunosuppression and another had acute promyelocytic leukemia, apart from their previous COVID-19 positive status.

Out of these 58 cases, 47 patients i.e., 81% had documented deranged blood glucose levels during the COVID-19 episode or thereafter.

Proportion of study patients with deranged blood glucose levels is demonstrated in Supplementary Figure 2.

Paranasal Sinus involvement:

Ethmoid sinus (57/58 i.e., 98.3%) was found to be the most frequently involved sinus [Figure 3]. Here, bilateral involvement (49/58 i.e., 84.5%) was more common than unilateral involvement.

This was followed by maxillary sinus involvement. Amongst the turbinates, the middle turbinate was found to be the most frequently involved. This is demonstrated in Figure 2.

Masticator space and adjacent structure involvement is tabulated in [Table 3]

Pterygomaxillary fissure (37/58 i.e., 64.0%) and pterygopalatine fossa (33/58 i.e., 56.9%) were equally involved on the right and the left. Unilateral involvement of the pterygomaxillary fissure is much more common than bilateral involvement.

The most commonly involved muscle in the masticator space was the medial pterygoid muscle.

The retro-antral fat pad was also nearly equally affected on both sides namely 21/58 on the right side and 20/58 on the left side.

Subcutaneous tissue involvement:

Subcutaneous extension into the premaxillary fat or the preseptal region of the orbit was seen in 40/58 i.e.,70% of cases.

Parotid gland involvement was seen in a single case.

Perineural spread was seen in 11 cases (19%) and the left mandibular nerve (8/58 cases i.e., 13.8% cases) was found to be the most common nerve demonstrating perineural spread (Figure 3).

Orbital invasion:

Orbital invasion was found to be predominantly in the extraconal space on the medial aspect (36 /58 i.e., 62.1%) followed by the inferior aspect (30/58 i.e., 51.7%) Unilateral involvement was found to be far more common than bilateral involvement.

Correspondingly, the most commonly involved intraocular muscles were also found to be the medial rectus (38 i.e., 65.5%), and the inferior rectus muscles (23 i.e., 39.7%) closely followed by the superior rectus (21/58 i.e., 36%). Involvement of orbit and related structures is elaborated in Table 4.

Table 4
Masticator space involvement

STRUCTURE	RIGHT	LEFT	BOTH
PTERYGOMAXILLARY FISSURE	18	18	1
PTERYGOPALATINE FOSSA	16	16	1
RETROANTRAL FAT	21	20	2
PTERYGOID PLATE	16	16	1
MEDIAL PTERYGOID MUSCLE	18	13	1
LATERAL PTERYGOID MUSCLE	17	14	1
TEMPORALIS MUSCLE	14	16	1
SUBCUTANEOUS PLANE	20	18	2

Orbital abscess was also seen in one case which was later on drained surgically [Figure 4].

Intracranial Findings:

31 patients out of 58 i.e., 53.4% were found to have intracranial invasion.

Pachymeningeal enhancement (28/31 i.e., 90.3%) was found to be the most common observation indicating intracranial invasion.

Infarcts (17/31 i.e., 55%) were the second most common finding indicating intracranial invasion. Amongst the cases with infarcts, four were watershed territory infarcts occurring in cases with complete ICA thrombosis [Figure 5].

Cavernous sinus thrombosis (11/58 i.e., 18.90%) [Figure 6] and Internal Carotid artery involvement (11/58) were also seen. Amongst the cases with internal carotid artery involvement, 8/11 i.e., 72.7% had complete thrombosis of the Internal carotid artery right from the origin. 3/11(27.2%) cases showed Internal carotid artery wall thickening, enhancement, and narrowing [Figure 7].

Fungal intraparenchymal abscesses [Figure 8] or changes of cerebritis were more common than fungal extra-axial abscesses. Intraventricular exudates were also seen in two cases in the dependant portion with restricted diffusion on DWI. i.e., the occipital horn of both lateral ventricles.

Extra-axial Haemorrhage in the form of subdural and subarachnoid hemorrhage and intraparenchymal hemorrhage [Figure 9] was seen in two and four cases respectively. Hence, A total of 5/31 i.e., 16.13% cases showed hemorrhagic changes.

Frequency distribution of intracranial findings and other manifestations in the study group is demonstrated in Table 5.

Table 5
Involvement of orbital and related structures

STRUCTURES INVOLVED	RIGHT	LEFT	BOTH
EXTRACONAL FAT	17	21	6
INTRACONAL FAT	12	16	7
INFRAORBITAL NERVE	5	12	13
APEX	10	17	4
OPTIC NERVE	10	16	3
LAMINA PAPYROCEA	14	13	4
CRIBRIFORM PLATE	22		
PANOPHTHALMITIS	2	1	0
ORBITAL ABSCESS	0	1	0

Cohen’s kappa coefficient for the inter-rater agreement was assessed for various parameters including the optic nerve involvement and cavernous sinus thrombosis was 0.7 suggestive of substantial inter-rater agreement all other findings had a Cohen’s coefficient value of 0.8-0.9 suggestive of near-perfect agreement. [8]

Discussion

The focus of this study was on the intracranial and orbital manifestations of COVID-19 associated with Rhino-cerebral mucormycosis. The role of MRI in the evaluation of mucormycosis has been well described previously. [9, 10]

Early signs of mucormycosis include the presence of non-enhancing turbinates, described as the black turbinate sign. [11, 12] Similar findings were also seen in our study [Figure 9].

Our findings included a significantly heterogeneous appearance within the involved sinuses, including T1 isointensity or hyperintensity, as well as T1/T2 hypointensity or isointensity [Figure 1].

Patients suffering from diabetes have already been known to be more prone to mucormycosis. [4] The European registry of patients with mucormycosis has also revealed a strong association between mucormycosis and diabetes as well as corticosteroid use. [13, 14] There is also evidence of an association between diabetes and SARS COV-2, including triggering of diabetic ketoacidosis. [15, 16] COVID-19 disease itself may also predispose to invasive fungal infections, especially of the sinuses. [17, 18] By demonstrating the association of these conditions, this study gives objective clues regarding the sudden surge in mucormycosis cases. [19]

Prior to the COVID-19 pandemic also, mucormycosis had a higher incidence in the Indian subcontinent than in any other region of the world, probably related to the higher burden of diabetes in India. [20] Susceptibility to Rhino-orbito-cerebral mucormycosis in COVID-19 patients is a consequence of decrease in phagocytic activity and an increase in the accessible iron. Protons in in diabetic ketoacidosis stimulate a transferrin-mediated displacement of iron. Fungal haeme oxygenase promotes iron absorption for fungal growth. This iron dependence also explains the angioinvasive propensity of fungal pathogens. [21]

Our study also included a case of post-COVID Rhinocerebral mucormycosis in a patient with history of solid organ transplantation as well as one with a haemo-lymphatic malignancy. [22] Similar phenomena have been documented previously. [23, 24, 14] However, this has rarely been reported in a post-COVID-19 context. [22]

Our study predominantly utilized MRI for the evaluation of rhino-cerebral mucormycosis. MRI not only possesses excellent soft-tissue resolution but is also free from ionizing radiation. MRI is more likely to be safe in the evaluation of these patients because patients with mucormycosis often need administration of nephrotoxic drugs. [12] CT was reviewed only in cases where it was needed to retrospectively evaluate the bony structures, and to help distinguish between susceptibility due to hemorrhage versus susceptibility due to fungal elements. But it was only rarely needed in our study. Our study also revealed a large number of cases in which there was spread of the disease without underlying bone erosion. This is because the intrinsic pathway of spread is along blood vessels or nerves and does not necessarily require bone erosion. Skull base osteomyelitis is also well delineated on MRI [Figure 10].

There are several unanswered questions regarding the pathways of spread of mucormycosis. Mucormycosis initially involves the nasal mucosa. This is followed by spread to the paranasal sinuses (typically the ethmoid and maxillary sinuses), then the orbit, and ultimately the intracranial fossa. [25] Ethmoid sinuses were found to be most frequently involved in our study. This is in keeping with findings described in a recent study by S Sharma et al [26].

The frequency of involvement of structures may also help in determining the temporal evolution of the disease process. The direct pathways of invasion of various structures observed in our study, also help to advance the understanding of the pathogenesis of mucormycosis.

According to our study, the dominant pathway of spread of mucormycosis is across the ethmoidal air cells and the lamina papyracea into the orbit and then into the medial and inferior aspect of the extraconal fat. Subsequently, the medial and inferior rectus muscles are involved. However, the inferior aspect of the extraconal fat of the orbit may also be invaded across the orbital floor.

The superior rectus muscle is typically involved via the spread into the superior extraconal space. This is also mostly through the lamina papyracea and occasionally via the frontal bone from the frontal sinus through the superior wall of the orbit. Invasion of orbital apex following intraconal invasion may result in orbital apex syndrome [Figure 11]. Optic neuritis may ensue [Figure 12]. Invasion of the superior orbital fissure which contains cranial nerves III, IV, and VI, and branches of V1 and V2, may result in ophthalmoplegia, diplopia, paraesthesia, and loss of sensations in the corresponding territories of the cornea and face. All cases of cavernous sinus thrombosis in our study had associated orbital apex involvement (Figure 6). This is in keeping with common pathways of spread into the cavernous sinus. [25, 27] However, there were two cases in which there was posterior intraconal space and optic nerve involvement without any extraconal fat or extraconal muscle involvement. These cases had enhancing soft tissue along the inferior orbital fissure and pterygopalatine fossa, which was indicative of the spread of the disease from the ipsilateral pterygopalatine fossa and along the inferior orbital fissure into the orbit. [25]

There were also two cases in our study that showed direct invasion of the left orbital apex from the sphenoid sinus.

The major reservoir of mucormycosis is considered to be the pterygopalatine fossa. [25]

Pathways of intracranial spread most frequently included, the orbital apex [28] with cavernous sinus involvement spreading into the adjacent middle cranial fossa, medial to the anterior temporal lobe with pachymeningeal enhancement extra-axial and intraparenchymal abscesses in this region [Figure 8].

Another pathway of spread is across the cribriform plate and the basifrontal region (anterior cranial fossa extension), [29] causing subdural abscesses [Figure 14, Figure 15] and adjacent vasculitic infarcts as well as intraparenchymal abscesses.

All cases of intraparenchymal and extra-axial hemorrhages in our study were located in the basifrontal region [Figure 9]. Intracranial hemorrhage is probably due to mycotic aneurysms and angioinvasive disease. [30] We observed mycotic aneurysms in the cavernous ICA [Figure 13], as well as in the posterior cerebral artery.

We also observed contiguous involvement of the infraorbital nerve in 30/58 (51.7%) patients. This was found to cause widening of the infraorbital foramen. The disease spread was then found to be along the inferior orbital fissure progressing to the pterygo-palatine fossa. A few cases also showed extension across the foramen rotundum into the middle cranial fossa.

Intracranial extension into the posterior cranial fossa was also demonstrated with vasculitic infarcts in the left superior cerebellar artery territory. There was also a case of a right middle cerebellar peduncle abscess. This represented extension along the cisternal segment of right trigeminal nerve. Only a few reports have documented this phenomenon. [31, 6] This indicates a pathway of perineural spread of the disease directly into the posterior cranial fossa [Figure 16].

Diffusion restriction is often seen and helps in evaluating the extent of involvement of various structures including the optic nerve, orbital apex, and the intracranial spread [Figure 17]. [12]

Fungal abscesses may present with only peripherally restricted diffusion [Figure 8] or heterogeneous diffusion restriction within the abscesses. This variant is seen in our study and also has been described before by Rangarajan et al. and Gaviani et al. [32, 33]

Infarcts included vasculitic or embolic infarcts as well as watershed territory infarcts in cases of complete ICA thrombosis [Figure 5].

In previous studies on non-COVID associated mucormycosis, the most commonly documented findings in the intracranial extension of mucormycosis, apart from meningeal enhancement, have been intracranial infected soft tissue/abscesses in 50% patients with intracranial extension and infarcts only in 20% cases [10] Therakathu et al have demonstrated 31% involvement of intracranial structures out of which, 38% showed cerebritis or abscesses, and 30% cases showed infarcts. [11] In comparison, our study, where 31 cases showed intracranial involvement, demonstrated infarcts in 55% of cases and internal carotid artery thrombosis in 13.8% cases. This suggests a possibility of higher occurrence of arterial thrombotic events including carotid artery involvement and infarcts in COVID-19 associated mucormycosis.

We have only considered acute infarcts with diffusion restriction on DWI in our current study.

Given, the association of COVID-19 with various thrombotic phenomena and the findings of our study, the possibility of a higher frequency of thrombotic complications in COVID19 associated mucormycosis vis-à-vis the proportion of these complications in patients with mucormycosis alone, merits consideration.

All cases of infratemporal fossa involvement in our study also had ipsilateral pterygomaxillary fissure involvement. This corroborates the theory of spread into infratemporal fossa via the pterygomaxillary

fissure.

Panophthalmitis [Figure 17] and optic neuritis [Figure 12] are devastating complications of Rhinocerebral mucormycosis and may result in permanent blindness. Their imaging findings have been described in Table 2. Early detection and prompt management of these complications may help to preserve vision.

However, in some cases with panophthalmitis, orbital exenteration may be needed. Here too, MRI plays a crucial role in the decision-making process. [34]

Conclusion

It is of paramount importance for clinicians as well as radiologists especially in the setting of the COVID-19 pandemic to consider the possibility of rhino-cerebral mucormycosis and evaluate in-depth for its myriad of possible complications.

COVID-19 associated Rhinocerebral mucormycosis has a plethora of intracranial manifestations. MRI can by virtue of its superior soft-tissue resolution, it not only expedite the diagnosis of initial stages of mucormycosis and help in early diagnosis of its complications but can also guide the clinician by effectively mapping out the exact disease extent.

Given the findings of our study and the association of COVID-19 with various thrombotic phenomena, we propose the hypothesis that post-COVID mucormycosis may be associated with a larger number of acute infarcts in patients with intracranial involvement as compared to the intracranial complications occurring in patients of mucormycosis alone. This requires validation with larger studies and may have important therapeutic implications.

For meticulous reporting in cases of COVID-19 related mucormycosis and for timely diagnosis of its plethora of complications, radiologists must follow a structured reporting format. This not only permits rigorous evaluation of the scan but also expedites the reporting process.

Limitations

Lack of a control group. Hence odds ratios and relative risk cannot be estimated.

Abbreviations

COVID-19 Coronavirus Disease- 2019

MRI- Magnetic resonance imaging

CT- Computed tomography

FLAIR- Fluid Attenuated Inversion Recovery sequence

SWI- Susceptibility Weighted Imaging

DWI- Diffusion weighted Imaging

MPRAGE- Magnetization-Prepared Rapid Acquisition with Gradient Echo

TOF- Time of Flight

KOH-Potassium Hydroxide

ICA-Internal carotid artery

MIP- Maximum intensity projection

Declarations

Source(s) of support:

NA

Acknowledgments:

Nil

Meetings/ Presentations:

This original article has not been presented as a part of any meeting/ conference.

Financial support and sponsorship:

Nil

Conflicts of interest:

On behalf of all authors, the corresponding author states that there is no conflict of interest.

Nil.

Consent for participation and consent for publication:

Consent waiver obtained from institutional ethics committee (retrospective observational study)

Availability of data and material:

Available on request from the authors.

Ethics Approval:

Institutional Ethics Committee of Seth G S Medical College, KEM Hospital

Author's Contributions:

1) Dr.Megha Nair was involved in Conception and design, acquisition and analysis of the data in this case, drafting of the article and revising it critically for intellectual content and final approval of the version to be published.

2) Dr. Shilpa Sankhe was involved in conception and design of this manuscript, analysis of the data, drafting of the article, revising it critically for intellectual content and final approval of the version to be published.

3) Dr. Gayatri Autkar was involved in conception and design of this manuscript, analysis of the data, revising the article critically for intellectual content and final approval of the version to be published.

References

1. Wang C, Wang Z, Wang G. COVID-19 in early 2021 : current status and looking forward. Signal Transduct Target Ther [Internet]. 2021;(February). Available from: http://dx.doi.org/10.1038/s41392-021-00527-1
2. Jain VK, Iyengar KP, Vaishya R. Differences between First wave and Second wave of COVID-19 in India. Diabetes Metab Syndr Clin Res Rev [Internet]. 2021; Available from: https://www.sciencedirect.com/science/article/pii/S1871402121001478
3. Spellberg B. Gastrointestinal mucormycosis: An evolving disease. Gastroenterol Hepatol. 2012;8(2):140–2.
4. Chikley A, Ben-Ami R, Kontoyiannis DP. Mucormycosis of the central nervous system. J Fungi. 2019;5(3):1–20.
5. Manesh A, Rupali P, Sullivan MO, Mohanraj P, Rupa V, George B, et al. Mucormycosis-A clinicoepidemiological review of cases over 10 years. Mycoses. 2019 Apr;62(4):391–8.
6. Herrera A, Dublin AB, Ormsby EL, Aminpour S, Howell LP. Imaging Findings of Rhinocerebral Mucormycosis. 2009;1(212):117–25.
7. Mehta S, Pandey A. Rhino-Orbital Mucormycosis Associated With. 2020;12(9):10–4.
8. McHugh ML. Interrater reliability: the kappa statistic. Biochem medica [Internet]. 2012;22(3):276–82. Available from: https://pubmed.ncbi.nlm.nih.gov/23092060
9. Carpenter JS, Roberts TD, Bailey N. The " Black Turbinate " Sign : An Early MR Imaging Finding of Nasal Mucormycosis. 2010;
10. Mohindra S, Mohindra S, Gupta R, Bakshi J, Gupta SK. Rhinocerebral mucormycosis: The disease spectrum in 27 patients. Mycoses. 2007;50(4):290–6.
11. Therakathu J, Rupa V, Prabhu S, Irodi A, Sudhakar SV, Yadav VK. The Egyptian Journal of Radiology and Nuclear Medicine Imaging features of rhinocerebral mucormycosis : A study of 43 patients.

Egypt J Radiol Nucl Med [Internet]. 2018;49(2):447–52. Available from: https://doi.org/10.1016/j.ejrnm.2018.01.001

12. Lone PA, Wani NA, Jehangir M. Rhino - orbito - cerebral mucormycosis : Magnetic resonance imaging. 2015;21(3):10–3.
13. Skiada A, Pagano L, Groll A, Zimmerli S, Dupont B, Lagrou K, et al. Zygomycosis in Europe: Analysis of 230 cases accrued by the registry of the European Confederation of Medical Mycology (ECMM) Working Group on Zygomycosis between 2005 and 2007. Clin Microbiol Infect [Internet]. 2011;17(12):1859–67. Available from: http://dx.doi.org/10.1111/j.1469-0691.2010.03456.x
14. Al-Ajam MR, Bizri AR, Mokhbat J, Weedon J, Lutwick L. Mucormycosis in the Eastern Mediterranean: a seasonal disease. Epidemiol Infect [Internet]. 2006 Apr;134(2):341–6. Available from: https://pubmed.ncbi.nlm.nih.gov/16490139
15. Paul A, Sainath D, Srikanth K. COVID - 19 and orbital mucormycosis. 2020;69(4):1002–4.
16. Gangneux J-P, Bougnoux M-E, Dannaoui E, Cornet M, Zahar JR. Invasive fungal diseases during COVID-19: We should be prepared. J Mycol Med [Internet]. 2020;30(2):100971. Available from: https://www.sciencedirect.com/science/article/pii/S115652332030069X
17. Fignani D, Licata G, Brusco N, Nigi L, Grieco GE, Marselli L, et al. SARS-CoV-2 Receptor Angiotensin I-Converting Enzyme Type 2 (ACE2) Is Expressed in Human Pancreatic β-Cells and in the Human Pancreas Microvasculature. Front Endocrinol (Lausanne). 2020;11(November):1–19.
18. Gazzaz ZJ. Diabetes and COVID-19. Open life Sci [Internet]. 2021 Mar 25;16(1):297–302. Available from: https://pubmed.ncbi.nlm.nih.gov/33817321
19. Garg D, Muthu V, Sehgal IS, Ramachandran R, Kaur H, Bhalla A, et al. Coronavirus Disease (Covid-19) Associated Mucormycosis (CAM): Case Report and Systematic Review of Literature. Mycopathologia [Internet]. 2021;186(2):289–98. Available from: http://europepmc.org/abstract/MED/33544266
20. Prakash H, Chakrabarti A. Epidemiology of Mucormycosis in India. Microorganisms. 2021 Mar;9(3).
21. Ibrahim AS, Spellberg B, Walsh TJ, Kontoyiannis DP. Pathogenesis of Mucormycosis. 2012;54(Suppl 1):1–7.
22. Arana C, Cuevas Ramírez RE, Xipell M, Casals J, Moreno A, Herrera S, et al. Mucormycosis associated with covid19 in two kidney transplant patients. Transplant infectious disease : an official journal of the Transplantation Society. Denmark; 2021. p. e13652.
23. Siddiqi SU, Freedman JD. Isolated central nervous system mucormycosis. South Med J. 1994 Oct;87(10):997–1000.
24. Nautiyal A, Gadde A, Mahapatra AK, Bansal SB. Case Report A Case Report of Central Nervous System Mucormycosis and Aspergillus Pneumopericardium in a Renal Transplant Recipient. 2020;2020–2.
25. Hosseini SMS, Borghei P. Rhinocerebral mucormycosis: Pathways of spread. Eur Arch Oto-Rhino-Laryngology. 2005;262(11):932–8.

26. Sharma S, Grover M, Bhargava S, Samdani S, Kataria T. Post coronavirus disease mucormycosis: a deadly addition to the pandemic spectrum. 2021;(May).
27. Pelton RW, Peterson EA, Patel BC, Davis K. Successful treatment of rhino-orbital mucormycosis without exenteration: the use of multiple treatment modalities. Ophthal Plast Reconstr Surg. 2001 Jan;17(1):62–6.
28. Eprin BREW, All WAAH, Oodman JEG. Long-term survival in rhinocerebral mucormycosis. 1998;88:570–5.
29. Balai E, Mummadi S, Jolly K, Darr A, Aldeerawi H. Rhinocerebral Mucormycosis: A Ten-Year Single Centre Case Series. 2020;12(11).
30. Hilary LP, Mcwilliams S, Mellnick VM, Lubner MG, Pickhardt PJ, Menias CO. Imaging Spectrum of Invasive Fungal and Fungal-like Infections 1. 2017;(1).
31. Maheshwari S, Patil M, Shendey S. Mucormycosis creeping along the nerves in an immunocompetent individual. 2019;13(10):1–10.
32. Rangarajan K. MRI in central nervous system infections: A simplified patterned approach. World J Radiol. 2014;6(9):716.
33. Gaviani P, Schwartz RB, Hedley-Whyte ET, Ligon KL, Robicsek A, Schaefer P, et al. Diffusion-weighted imaging of fungal cerebral infection. Am J Neuroradiol. 2005;26(5):1115–21.
34. Shah K, Dave V, Bradoo R, Shinde C. Orbital Exenteration in Rhino-Orbito-Cerebral Mucormycosis: A Prospective Analytical Study with Scoring System. Indian J Otolaryngol Head Neck Surg [Internet]. 2019;71(2):259–65. Available from: https://doi.org/10.1007/s12070-018-1293-8

Figures

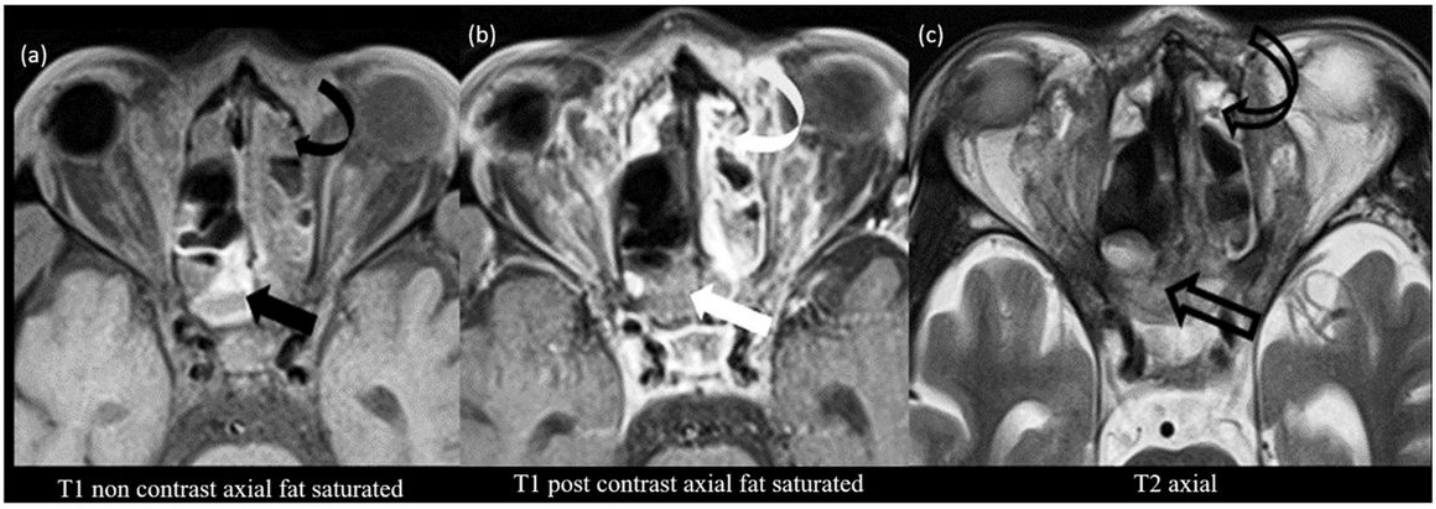

Figure 1: (a) T1 hyperintense (Black Arrow) and isointense (Curved black Arrow) sinus contents (b) Contrast enhanced image shows variable enhancement. White curved arrow) (c) T2 hypointense to isointense sinus contents (Hollow Arrow) and T2 hyperintense regions (Curved Hollow Arrow)

Figure 1

See image above for figure legend.

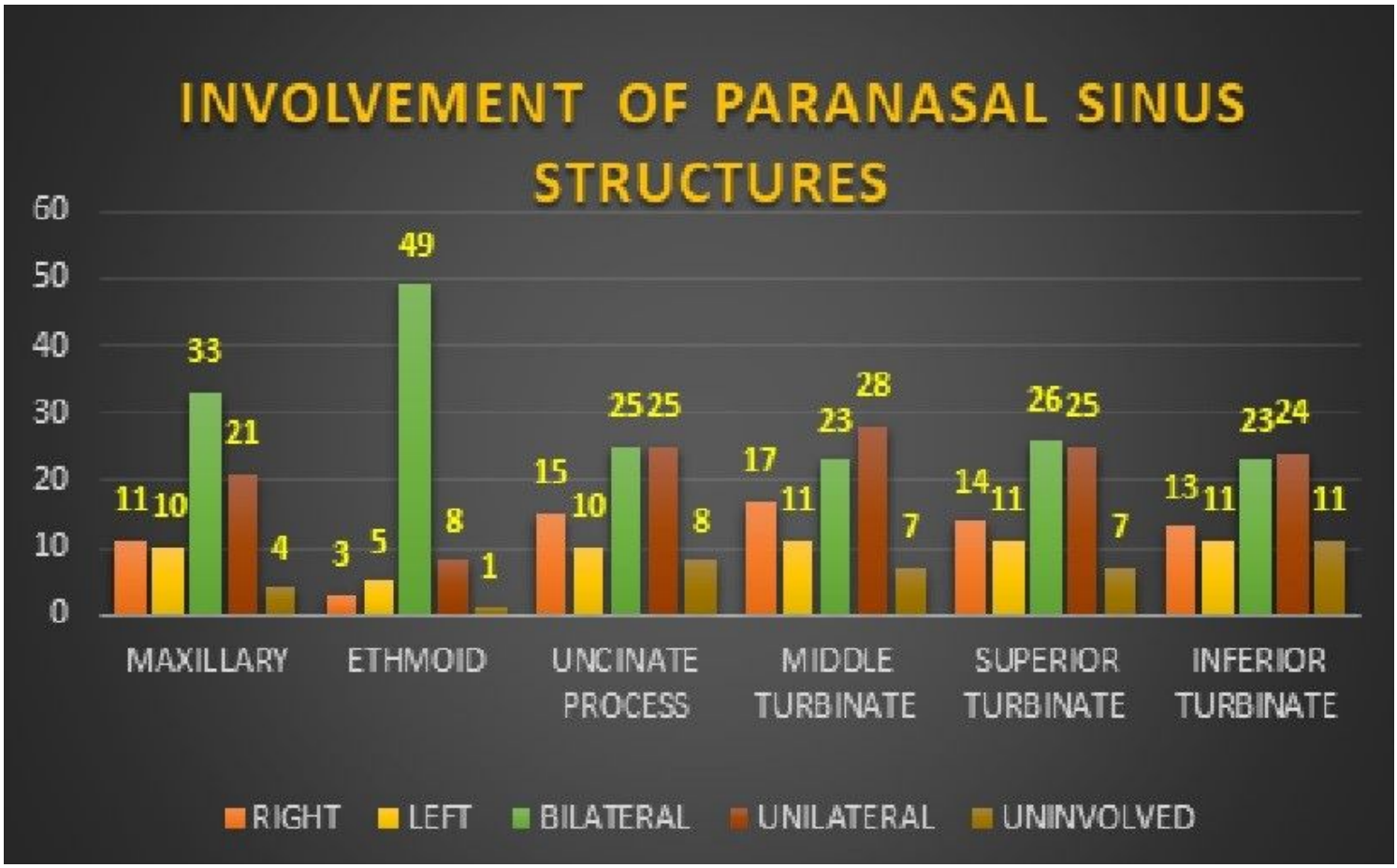

Figure 2

Bar diagram representing the involvement of various paranasal sinus structures

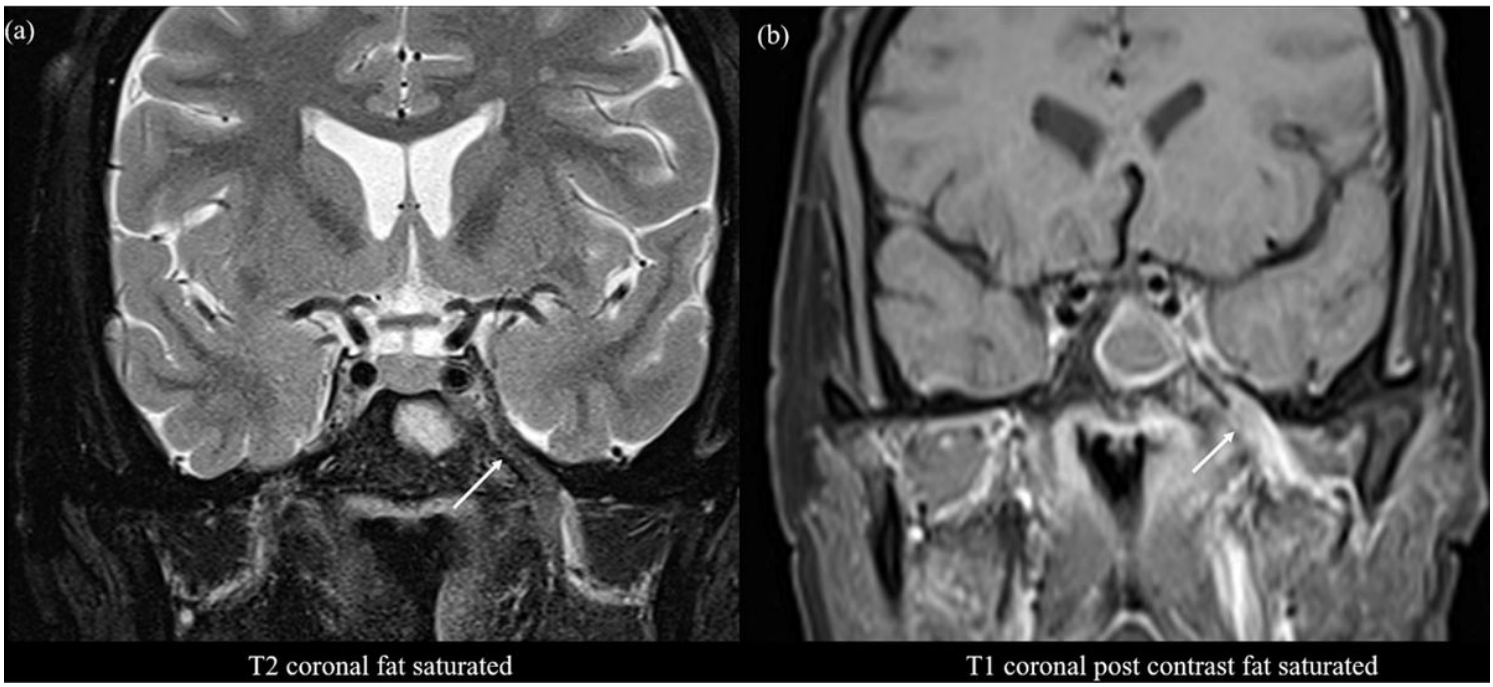

Figure 3

(a) Left trigeminal nerve shows T2 hypointensity along the left mandibular nerve with (b) post contrast enhancement along the nerve seen extending across the foramen ovale from the left masticator space to the cavernous sinus

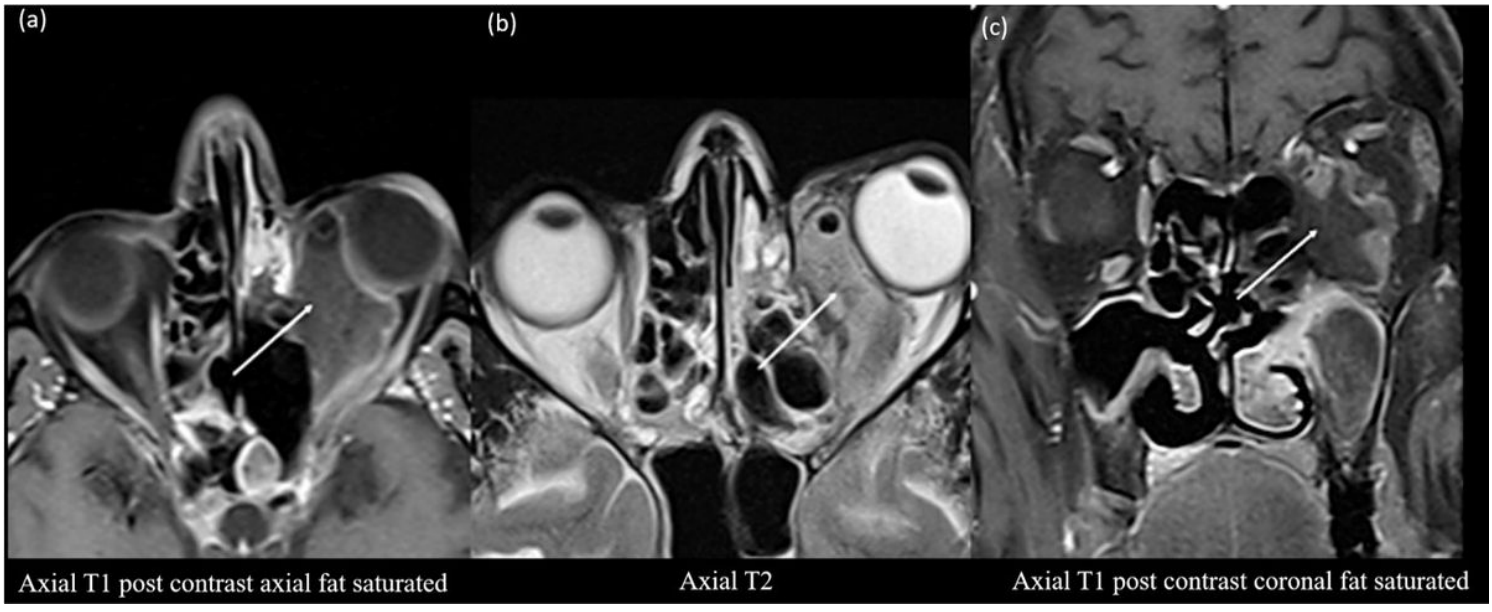

Figure 4

(a) Peripherally enhancing centrally necrotic/ non-enhancing abscess in the medial aspect of left orbit, (b) with heterogenous signal intensity on T2 due to fungal elements (c) Coronal view demonstrating the

orbital abscess.

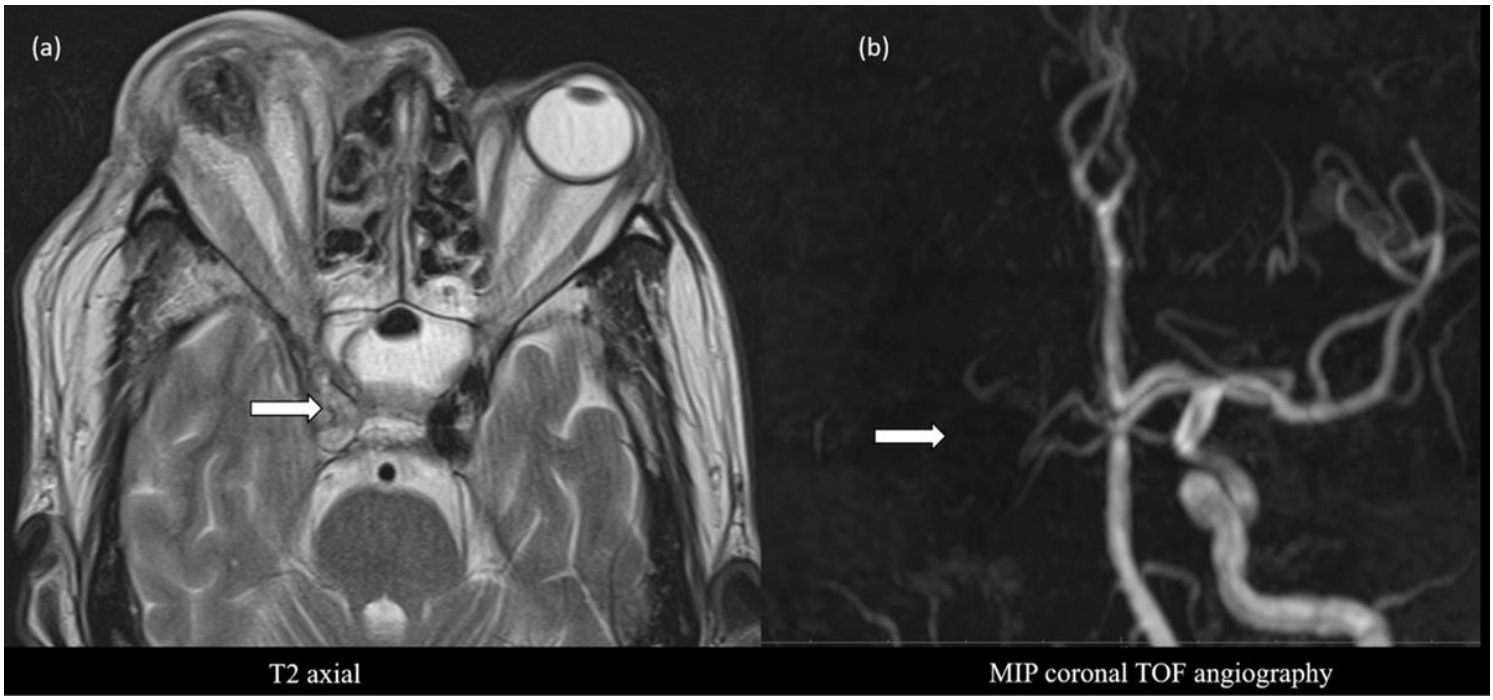

Figure 5

(a) Absence of right cavernous ICA flow void (b) Coronal MIP image of TOF angiography shows absence of flow related enhancement of right MCA and ICA in its entire extent suggestive of thrombosis. Note the right orbital involvement with panophthalmitis

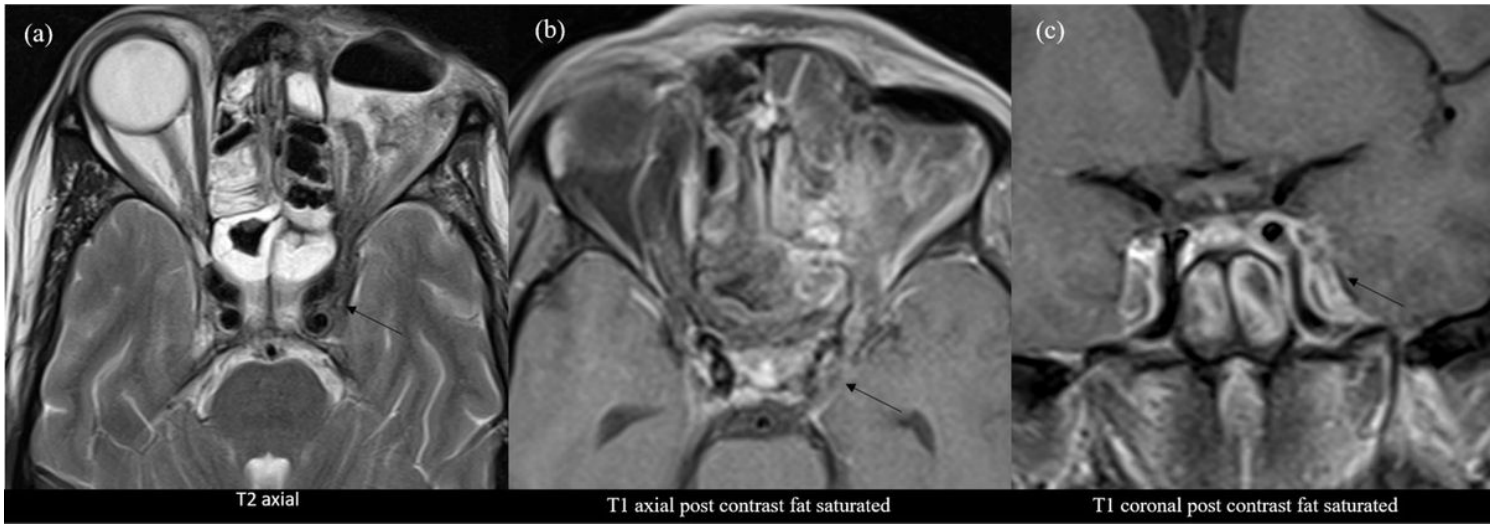

Figure 6

(a) Bulging lateral walls of the cavernous sinus with T2 hypointense contents within.

(b) Filling defects within the left cavernous sinus on the post contrast axial sections and (c) post contrast coronal sections respectively.

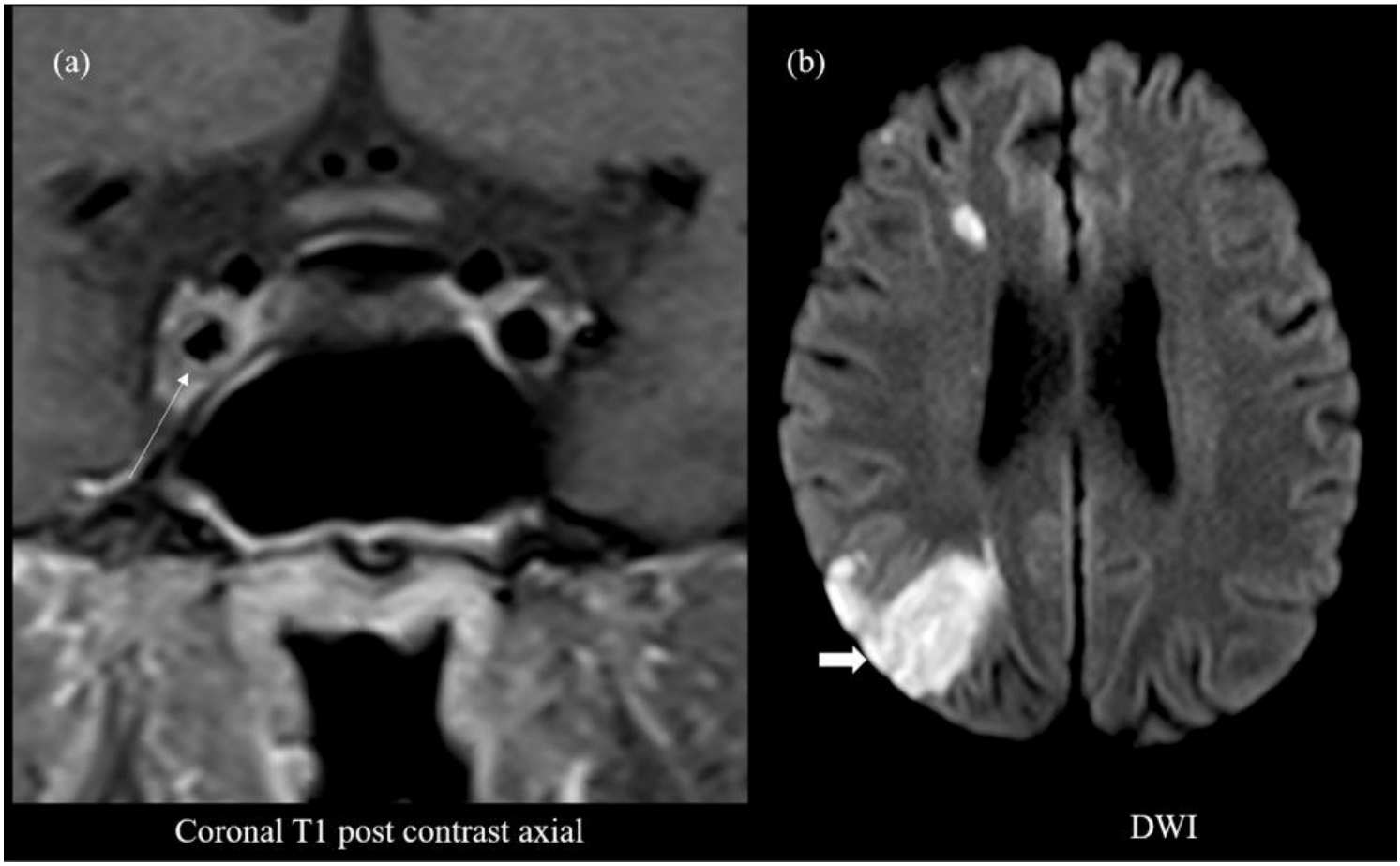

Figure 7

(a) Angioinvasive disease involving the right cavernous ICA causing ICA wall enhancement, luminal irregularity and luminal narrowing. (b) Acute infarcts showing diffusion restriction on DWI in the right MCA territory.

Figure 8

(a)Post contrast ring enhancing intraparenchymal collection in the left temporal lobe with (b) central T2 hyperintensity and hypointense fungal elements with (c) a peripheral rim of diffusion restriction (variant seen in fungal abscesses).

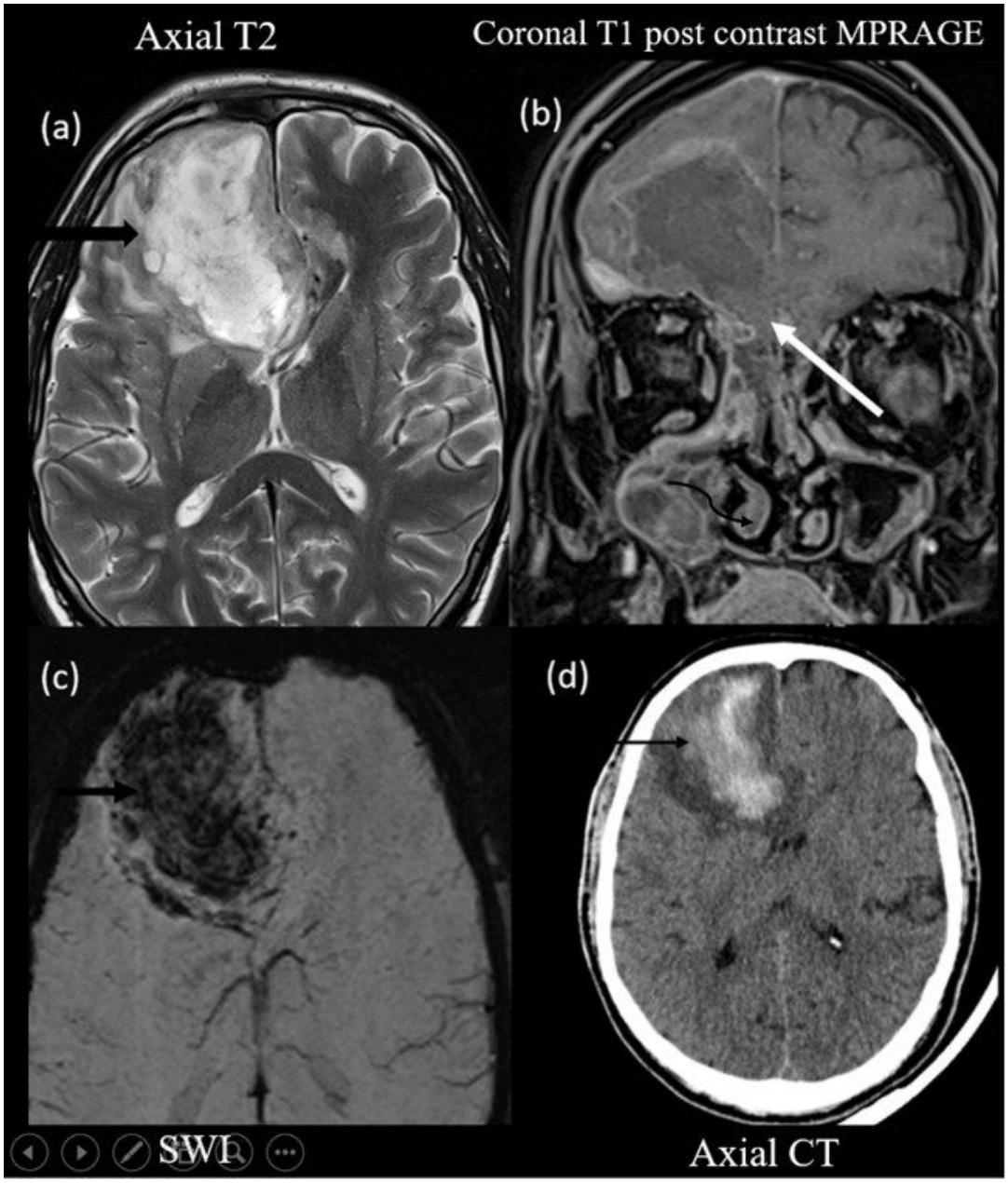

Figure 9: (a) Intraparenchymal hematoma (b) Direct intracranial invasion of the heterogeneously enhancing soft tissue across the cribriform plate is seen. Curved arrow points to "Black turbinate sign" ↘ (c) Susceptibility on SWI (d) CT confirms the presence of a hematoma (HU-55)

Figure 9

See image above for figure legend.

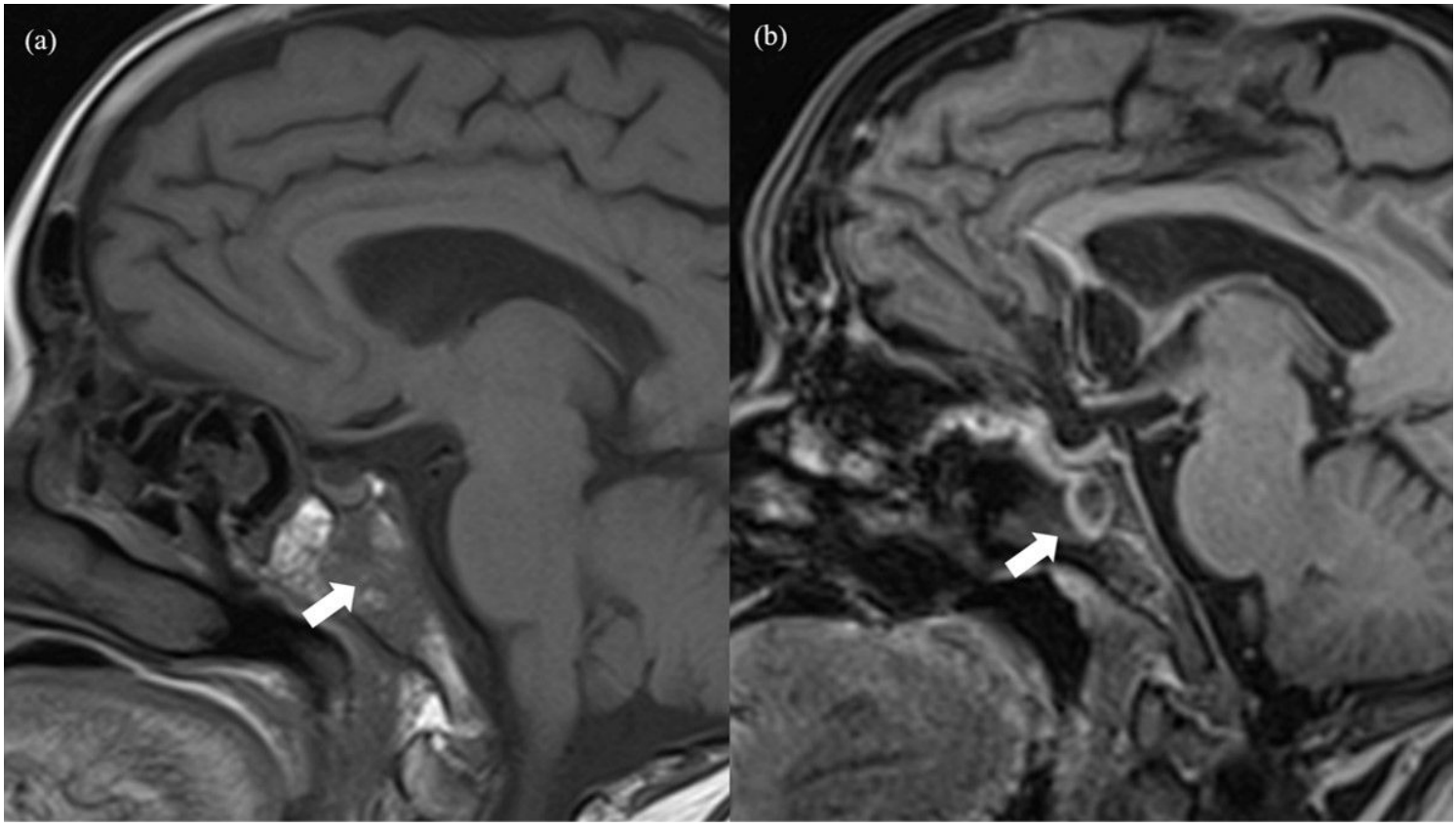

Figure 10

(a) Plain T1 non-fat saturated sagittal image showing hypointensity within the clivus (b) Post contrast sagittal T1 weighted MPRAGE image showing enhancing soft tissue in the clivus contiguous with the sphenoid sinus. This is suggestive of skull base osteomyelitis

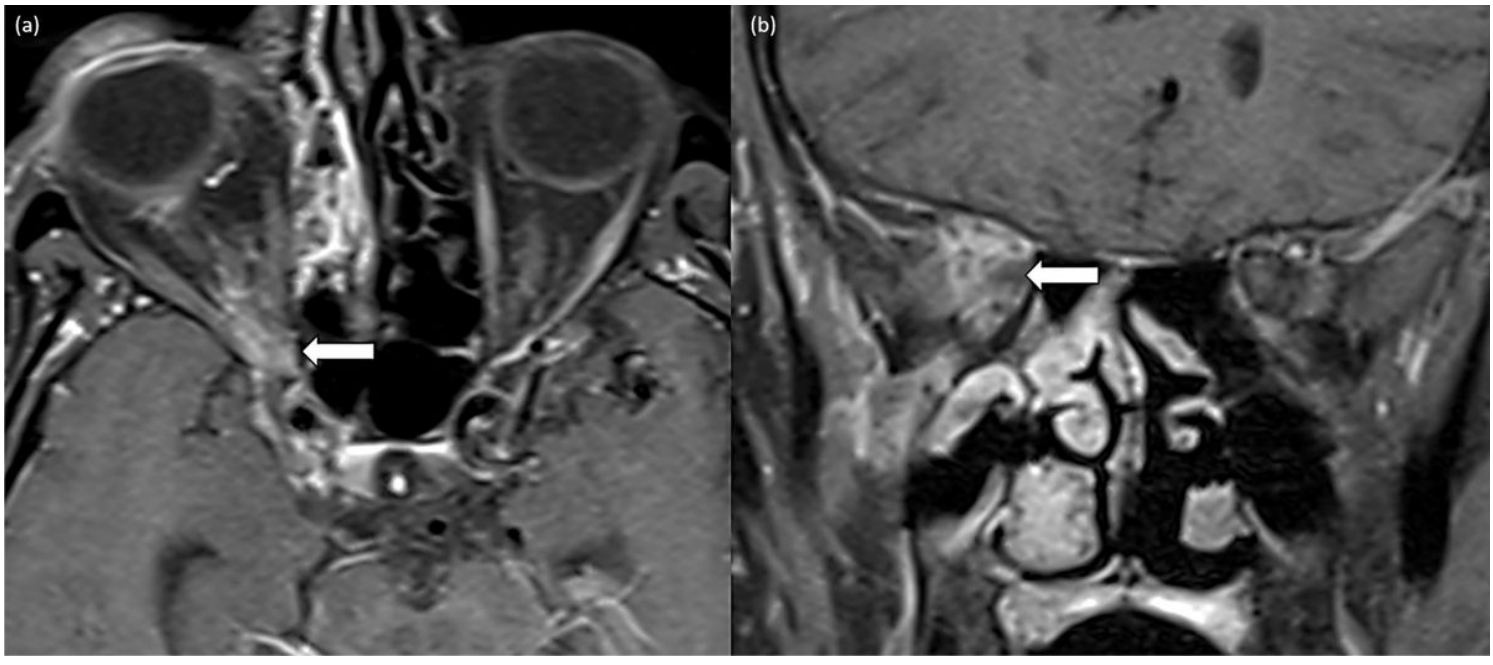

Figure 11

(a)Enhancing soft tissue in the right orbital apex on axial post contrast T1 fat saturated sequences extending into the right cavernous sinus. (b) Coronal view showing enhancing soft issue and crowding in the right orbital apex

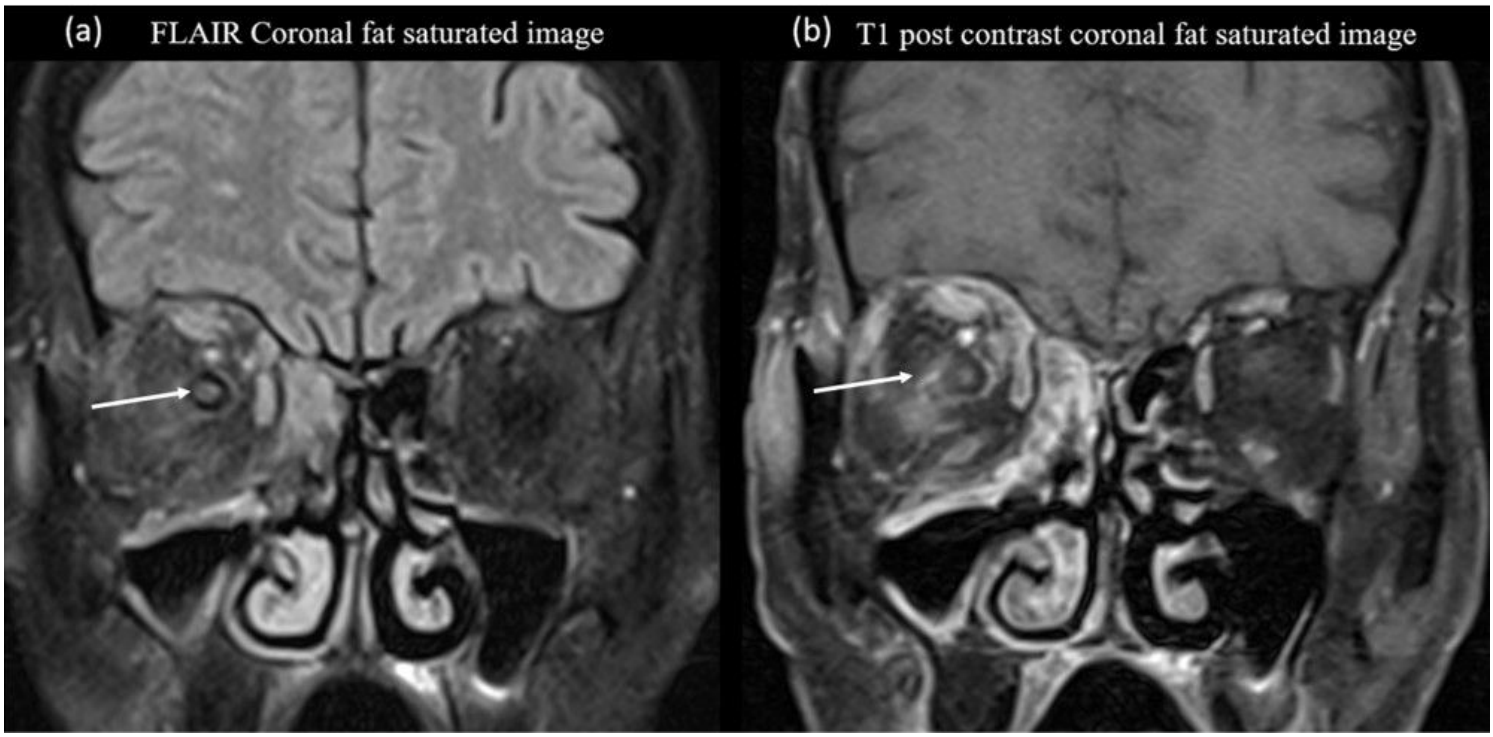

Figure 12

(a) FLAIR coronal image show hyperintensity within the right optic nerve and surrounding T2/FLAIR hyperintense inflammatory changes in the extraconal and intraconal compartments (b) The right optic nerve and surrounding structures show post contrast enhancement suggestive of optic neuritis

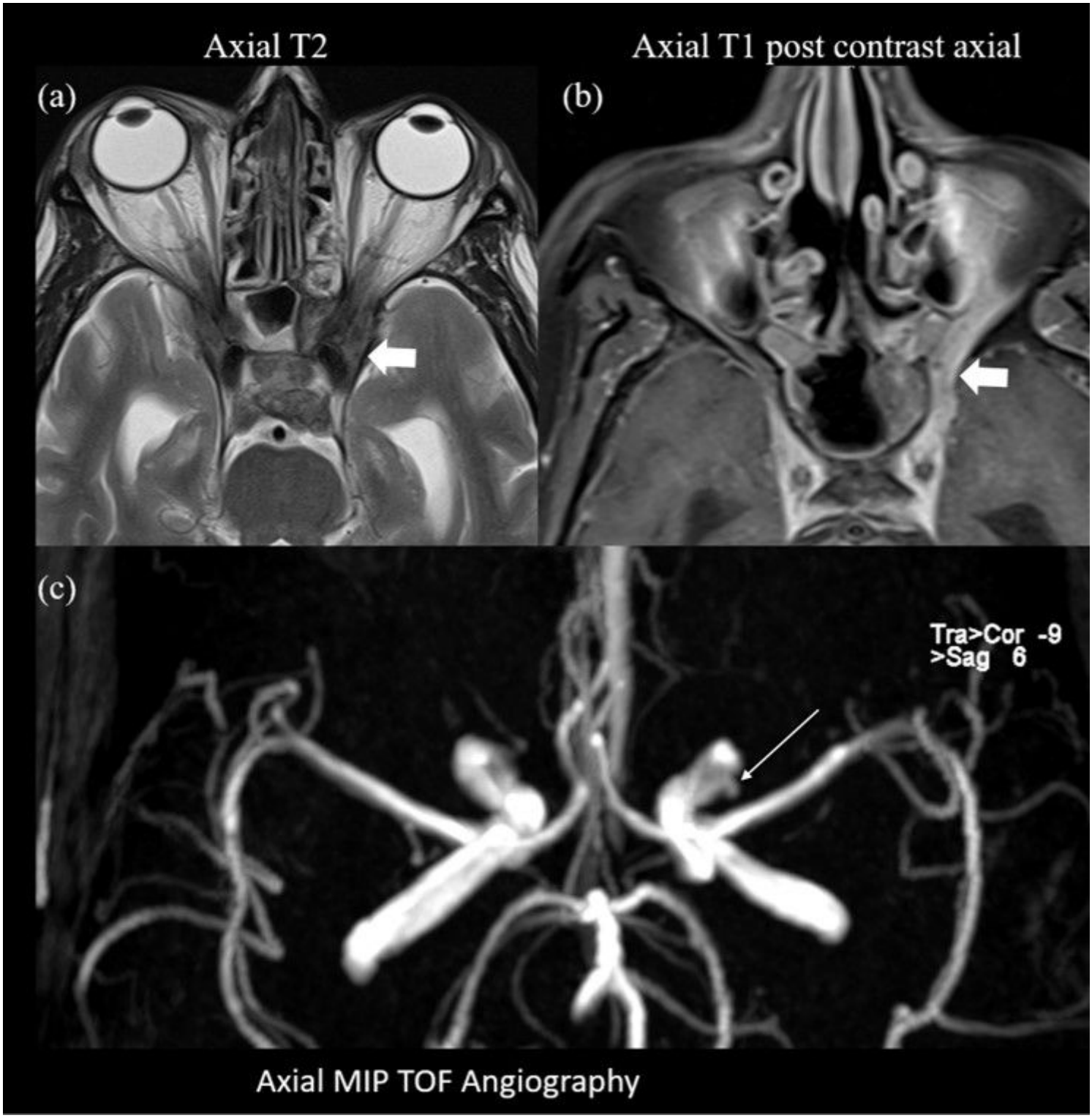

Figure 13

(a) Shows left orbital apex involvement as T2 hypointense contents (b) Postcontrast enhancement in the left orbital apex with invasion of left cavernous sinus (C) Small saccular mycotic aneurysm in the cavernous segment of left ICA.

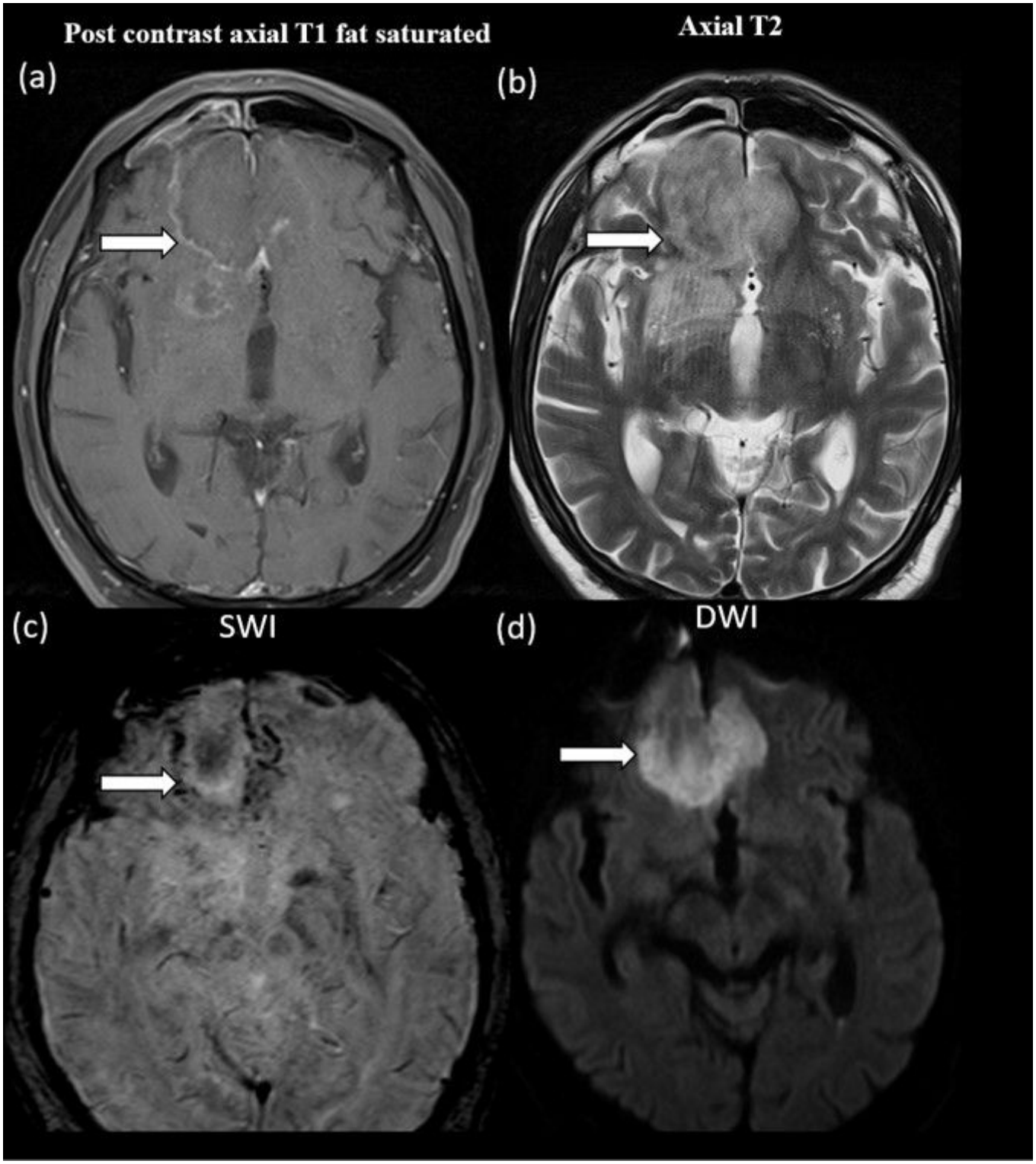

Figure 14

(a) Subdural peripherally enhancing abscess in basifrontal region (b) Heterogeneously hyperintense signal of the abscess contents (c) Susceptibility foci on SWI (likely to be due to fungal elements) (d) Central diffusion restriction on DWI

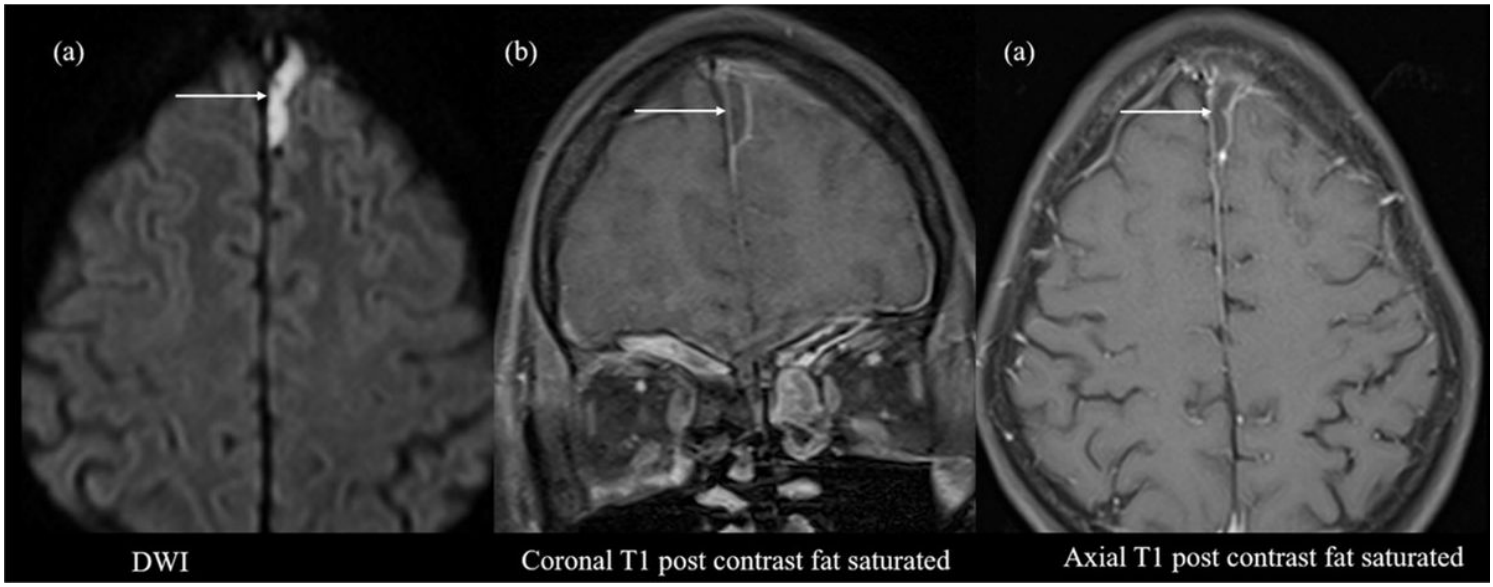

Figure 15

(a), (b) and (c) Parafalcine subdural peripherally enhancing collection that shows central diffusion restriction suggestive of a subdural empyema.

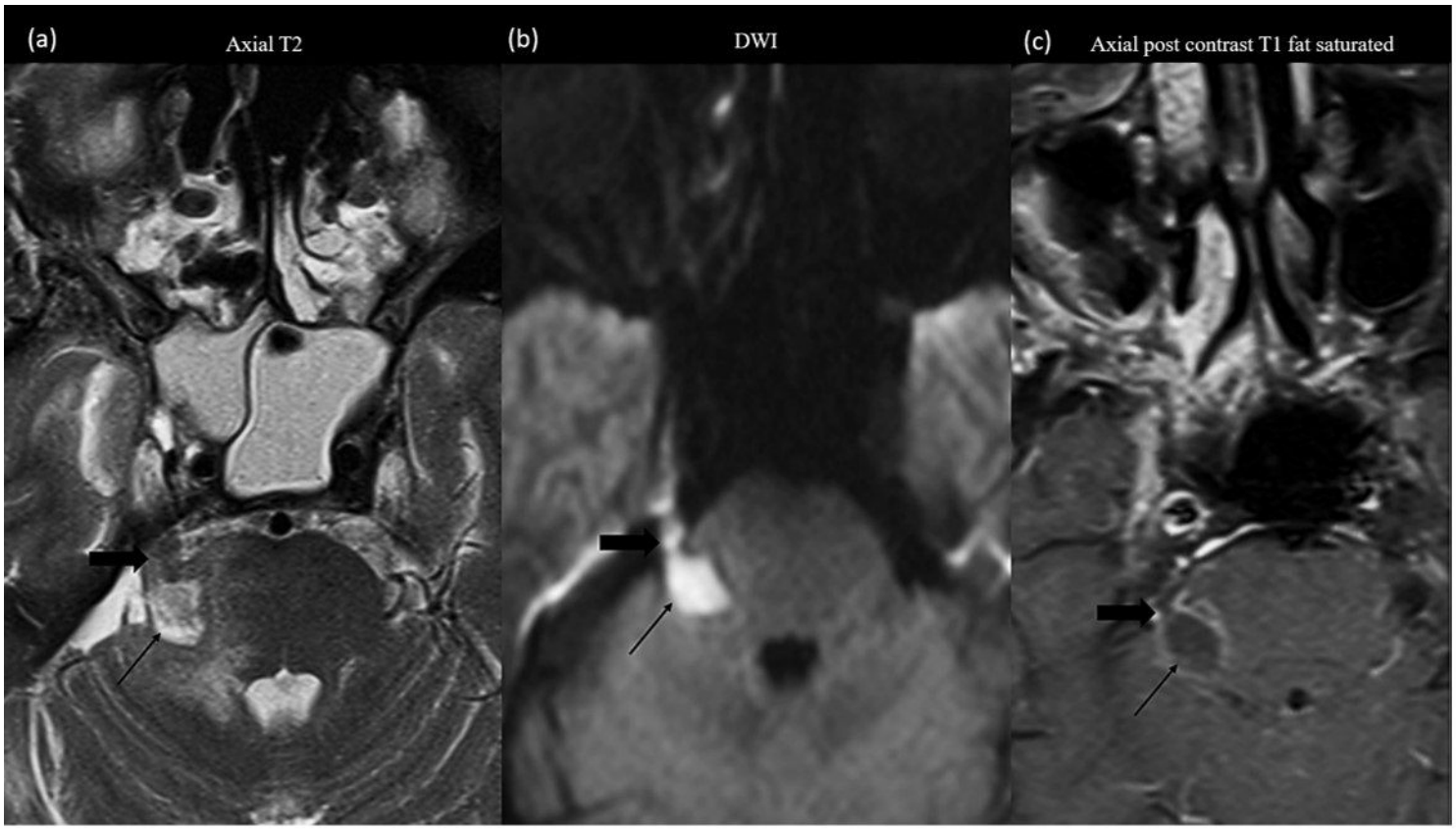

Figure 16: (a), (b) and (c) Perineural spread along the cisternal segment of the right trigeminal nerve (block arrow ➡) via cavernous sinus with peripherally enhancing abscess in the adjacent right hemipons showing central diffusion restriction (arrow ⟶)

Figure 16

See image above for figure legend.

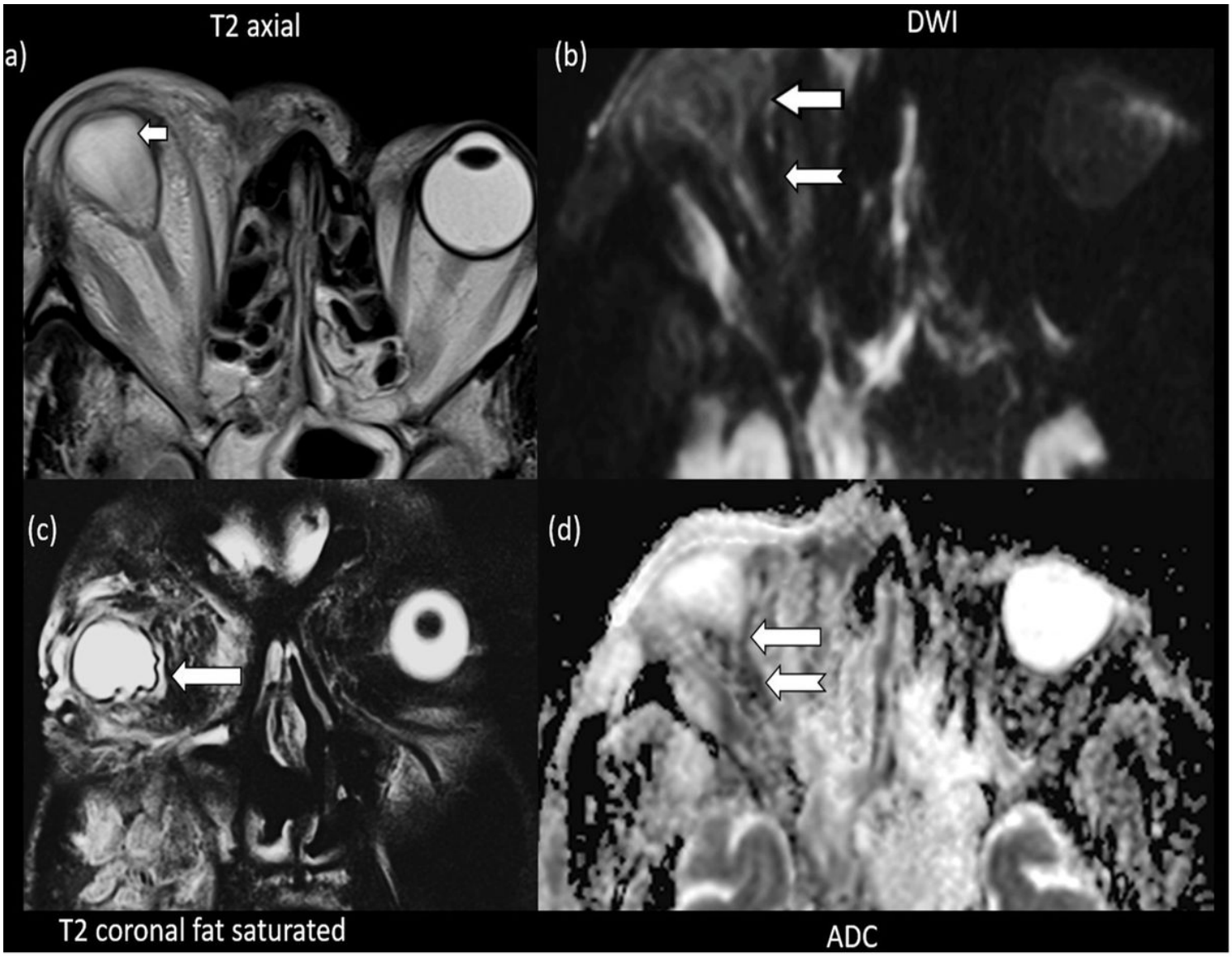

Figure 17: (a) Deformed globe and proptosis in a patient with panophthalmitis ⇦ (b) Posterior coats of the right eyeball ⇦ and right optic nerve ⇦ show diffusion restriction on DWI (c) Corresponding hypointensity in right eyeball ⇦ and optic nerve ⇦ on ADC weighted sequences

Figure 17

See image above for figure legend.

Supplementary Files

This is a list of supplementary files associated with this preprint. Click to download.

- Supplementarymaterial1.docx